

Asymmetric Small Molecule Acceptor for Organic Solar Cells with Short Current Density Over 24 mA cm⁻²

Fangfang Cai^{a‡}, Hongjian Peng^{a‡}, Honggang Chen^{a‡}, Jun Yuan^a, Jiefeng Hai^b, Tsz-Ki Lau^c, Ju
Wang^a, Yunbin Hu^a, Wei Liu^a, Xinhui Lu^c, Yingping Zou^{a*}

^a College of Chemistry and Chemical Engineering, Central South University, Changsha 410083,
China.

^bGuangxi Key Laboratory of Electrochemical and Magneto-
Chemical Functional Materials, College of Chemistry and Bioengineering, Guilin University of Te
chnology, Guilin 541004, Guangxi,
China

^c Department of Physics, The Chinese University of Hong Kong, New Territories, Hong Kong, P.
R. China

1 General Information	1
2 Experimental Section	2
2.1 Materials and Synthetic Procedures	2
2.2 Device Fabrication and Measurements	6
2.3 Optimization of Device Performance	9
2.4 Additional Information	11

1 General Information

^1H NMR and ^{13}C NMR spectra of intermediates and target small molecule were recorded on a Bruker Adv-400 spectrometer using d-chloroform as solvent at 293K. Chemical shift CHCl_3 ($\delta = 7.26$ ppm for ^1H NMR and $\delta = 77.0$ ppm for ^{13}C NMR). Multiplicities of NMR signal are described as s (signal) or m (multiplet). UV-Vis spectra were measured using a Shimadzu UV-2600 recording spectrophotometer. Cyclic voltammetry (CV) measurement of SMAs thin films were conducted on a CHI660E voltammetric analyzer in tetrabutylammonium hexafluorophosphate (Bu_4NPF_6 , 0.1 M) acetonitrile solutions as conventional three-electrode and using a scan rate of 20 mV s^{-1} . The morphologies of the PM6:Y22 blend films were investigated by atomic force microscopy (AFM, Agilent Technologies, 5500 AFM/SPM System, USA) in contacting mode with a $2 \mu\text{m}$ scanner. Transmission electron microscope (TEM) measurements were performed in a JEM-2100F.

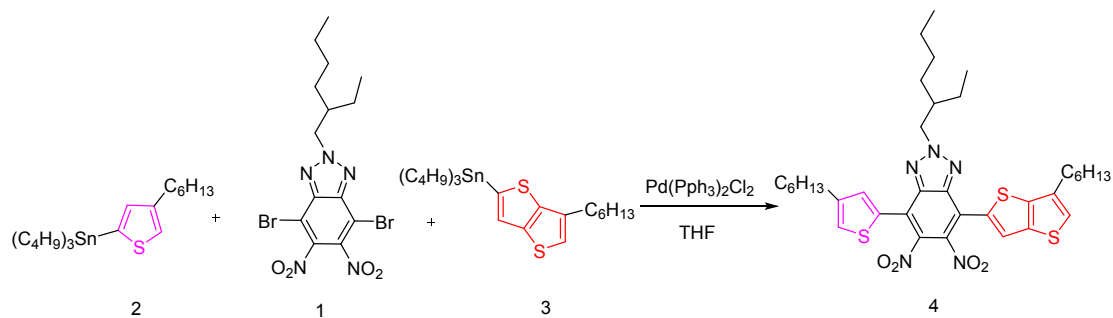
2 Experimental Section

2.1 Materials and Synthetic Procedures

Compound 1, compound 2 and compound 3 were synthesized according to the previous reported methods¹⁻³. The PBDB-T-2F (PM6), bis(triphenylphosphine)palladium(II) dichloride ($\text{Pd}(\text{PPh}_3)_2\text{Cl}_2$) and reagents were purchased from J&K and Alfa Asia Chemical Co. Tetrahydrofuran (THF) was further dried by using sodium under $110 \text{ }^\circ\text{C}$ refluxing condition. Compound 4 was synthesized by the stille-coupling reaction in one-pot method, but the pentacyclic, hexacyclic and heptacyclic products were obtained at same time, where the yield of

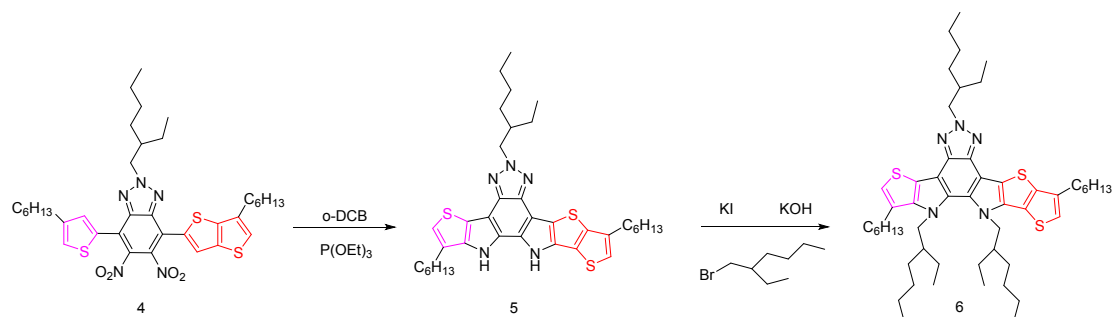
the target product compound 4 was not high.

Synthesis of 2-(2-ethylhexyl)-4-(6-hexylthieno[3,2-b]thiophen-2-yl)-7-(4-hexylthiophen-2-yl)-5,6-dinitro-2H-benzo[d][1,2,3]triazole (4)



Solution of compound 2 (3.58 g, 7.83 mmol), compound 3 (4.02 g, 7.83 mmol) and compound 1 (2.5 g, 5.22 mmol) was degassed in extra dry THF before, after which Pd(PPh₃)₂Cl₂ (0.24 g, 0.34 mmol) was added. After the mixture was refluxed under argon (Ar) for 24 hours, it was cooled to room temperature. The aqueous phase was extracted with dichloromethane. The solvent was removed under vacuum. Crude product was obtained as an orange liquid without further purification. The crude product was directly used for the next steps.

Synthesis of 5,11,12-tris(2-ethylhexyl)-1,8-dihexyl-11,12-dihydro-5H-thieno[2',3':4,5]pyrrolo[3,2-g]thieno[2',3':4,5]thieno[3,2-b][1,2,3]triazolo[4,5-e]indole (6)



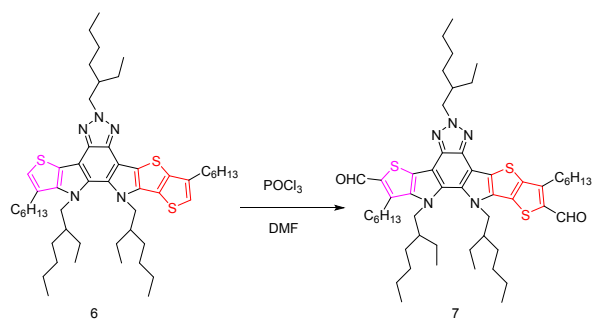
Compound 4 (3.25 g, 4.58 mmol) and triethyl phosphate (4 g, 24.2 mmol) was dissolved in extra dry *o*-dichlorobenzene (*o*-DCB, 60 mL) under nitrogen. After

refluxing at 180 °C for 12h, the reaction was cooled to room temperature. Crude product 5 was obtained as a dark green liquid without further purification. The crude product was directly used for the next step

Crude product (5), 1-bromo-2-ethylhexane (7.9 g, 41.22 mmol), potassium iodide (0.34 g, 1.8 mmol) and potassium carbonate (2.56 g, 45.8 mmol) were dissolved in N, N-dimethylmethanamide (DMF, 50 mL). After being heated at 90 °C overnight, the reaction was cooled down to room temperature. The solution was removed under vacuum and extracted with dichloromethane. The resulting mixture was purified with column chromatography on silica gel using dichloromethane/petroleum ether (1/8, v/v) as the eluent to give a light-yellow solid 6 (1.1 g, 25% yield).

¹H NMR (400 MHz, CDCl₃) δ 6.99 (s, 1H), 6.96 (s, 1H), 4.72 (d, *J* = 7.2 Hz, 2H), 4.59 (d, *J* = 6.4 Hz, 2H), 4.44 (d, *J* = 7.3 Hz, 2H), 2.91 (t, *J* = 7.5 Hz, 2H), 2.82 (t, *J* = 7.6 Hz, 2H), 2.44 – 2.22 (m, 1H), 2.20 – 2.14 (m, 1H), 1.92 – 1.79 (m, 5H), 1.49 – 1.16 (m, 24H), 1.10 – 0.70 (m, 28H).

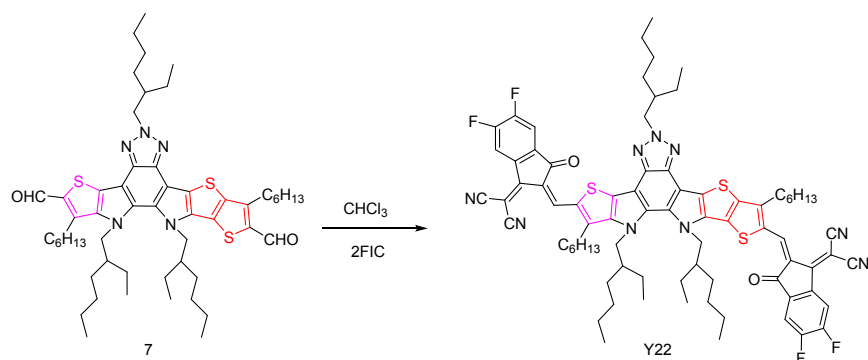
Synthesis of 5,11,12-tris(2-ethylhexyl)-1,8-dihexyl-11,12-dihydro-5H-thieno[2',3':4,5]pyrrolo[3,2-g]thieno[2',3':4,5]thieno[3,2-b][1,2,3]triazolo[4,5-e]indole-2,9-dicarbaldehyde (7)



To a solution of compound 6 (1.1 g, 1.26 mmol) in extra-dry DMF (80 mL) at 0 °C, phosphorus oxychloride (5 ml) was slowly added dropwise under Ar atmosphere. Then after stirring additional 2 h at 0°C, the solution was heated to 90 °C and stirred overnight. The reaction mixture was poured into water (500 mL), and then multiple extractions were performed by dichloromethane. After evaporating under reduced pressure, the crude product was purified by column chromatography (petroleum/dichloromethane = 5/1, v/v) to obtain compound 7 (0.725 g, 75%) as a yellow solid.

¹H NMR (400 MHz, CDCl₃) δ 10.07 (d, *J* = 1.3 Hz, 1H), 10.06 (s, 1H), 4.65 (d, *J* = 7.1 Hz, 2H), 4.54 (s, 2H), 4.38 (d, *J* = 6.9 Hz, 2H), 3.13 (t, *J* = 7.6 Hz, 4H), 2.49 2.04 (m, 1H), 2.13 – 1.66 (m, 6H), 1.83 – 0.36 (m, 60H).

Synthesis of 2,2'-((2*Z*,2'*Z*)-((5,11,12-tris(2-ethylhexyl)-1,8-dihexyl-11,12-dihydro-5H-thieno[2',3':4,5]pyrrolo[3,2-*g*]thieno[2',3':4,5]thieno[3,2-*b*][1,2,3]triazolo[4,5-*e*]indole-2,9-diyl)bis(methanylylidene))bis(5,6-difluoro-3-oxo-2,3-dihydro-1*H*-indene-2,1-diylidene))dimalononitrile (Y22)



Compound 7 (0.176 g, 0.19 mmol) and 2-(5,6-difluoro-3-oxo-2,3-dihydro-1*H*-inden-1-ylidene)malononitrile (2FIC) (0.2 g, 0.76 mmol), chloroform (50 mL) were dissolved in a round bottom flask under nitrogen. Then pyridine (1.26 mL) was slowly added dropwise. The solution was heated to 65 °C and stirred overnight. After the reaction was completed, the reaction was poured into 200 mL of methanol and the crude product was precipitated. The residue was extracted with methanol, n-hexane and chloroform for 12 h by using a soxhlet extractor. Finally, chloroform solution was removed by rotary evaporator. The residue was purified with column chromatography on silica gel using dichloromethane/petroleum ether (1.25/1, *v/v*) as the eluent to give a dark blue solid Y22 (0.79 g, 70% yield).

¹H NMR (400 MHz, CDCl₃) δ 9.21 (s, 1H), 9.16 (s, 1H), 8.62 – 8.52 (m, 2H), 7.71 (q, *J* = 7.1 Hz, 2H), 4.73 (d, *J* = 6.8 Hz, 4H), 4.51 (s, 2H), 3.32– 3.14 (m, 3H), 2.39 (d, *J* = 5.7 Hz, 1H), 1.87 (dd, *J* = 15.4, 7.7 Hz, 6H), 1.67 – 1.17 (m, 37H), 0.93 (dt, *J* = 21.3, 7.2 Hz, 25H).

¹³C NMR (101 MHz, CDCl₃) δ 186.08, 185.90, 159.52, 158.88, 155.59, 153.83, 153.01, 152.88, 145.99, 145.57, 144.08, 139.66, 138.78, 138.55, 136.68, 136.65, 136.60, 136.52, 136.06, 136.01, 135.95, 135.70, 135.49, 135.26, 134.57, 134.53, 134.45, 133.54, 132.76, 129.71, 119.97, 119.66, 115.47, 114.99, 114.94, 114.82,

114.74, 114.61, 113.72, 112.52, 112.33, 110.63, 68.67, 67.46, 59.97, 54.72, 54.09, 40.56, 40.39, 32.03, 31.62, 31.23, 30.50, 29.87, 29.51, 29.23, 28.41, 28.11, 24.01, 22.95, 14.12, 14.07, 14.02, 13.63, 10.54.

(MALDI-TOF) m/z calcd. for ($C_{78}H_{83}N_9O_2S_3$): 1349.58. Found: 1349.5754.

2.2 Device Fabrication and Measurements

2.2.1 Inverted solar cells

A ZnO sol-gel solution was prepared by dissolving $[Zn(CH_3COO)_2 \cdot 2H_2O]$ in 2-methoxyethanol containing ethanolamine as a stabilizer (the three reagents were purchased from Sigma-Aldrich Co.). The solution was 0.75 M in ZnO and was stirred for at least 6h using a magnetic stirrer to obtain a homogeneous solution. It was spin-coated onto ITO glass (3500 rpm for 40 s). The films were annealed at 150 °C in air for 1h. ZnO film thickness is ~30 nm. The active layer materials were dissolved in chloroform (CF) and spin-coated onto the ZnO layer. Thermal annealing treatment were performed under different temperatures or no thermal annealing treatment for the active layer. MoO_3 (~6 nm) and Ag (~80 nm) was successively evaporated onto the active layer through a shadow mask (pressure under ca. 10^{-4} Pa). The effective area for the devices is 5.0 mm². J - V curves were measured by using a computerized Keithley 2400 Source Meter and a Xenon-lamp-based solar simulator (Enli Tech, AM 1.5 G, 100 mW/cm²), calibrated by a standard silicon cell. J - V curves were recorded with a Keithley 236 digital source meter. The external quantum efficiency (EQE) spectra were measured by using a QE-R3011 measurement system (Enli Tech). All of

these fabrications and characterizations after spin-coated ZnO substrates were conducted in a glove box.

2.2.2 Conventional solar cells

The OSCs were fabricated in the configuration of the conventional structure with an indium tin oxide (ITO) glass as positive electrode and an ETL/Al as negative electrode. Patterned ITO glass with a sheet resistance of $10 \Omega/\text{sq}$ was purchased from CSG HOLDING Co. LTD. (China). The ITO glass was cleaned by sequential ultrasonic treatment in detergent, deionized water, acetone and isopropanol, and then treated in an ultraviolet-ozone chamber (Ultraviolet Ozone Cleaner, Jelight Company, USA) for 20 min. Then PEDOT:PSS (poly(3,4-ethylene dioxythiophene):poly(styrene sulfonate)) (Baytron PVP Al 4083, Germany) was filtered through a $0.45 \mu\text{m}$ poly(tetrafluoroethylene) (PTFE) filter and spin coated at 3000 rpm for 40 s on the ITO substrate. Subsequently, PEDOT: PSS film was baked at 150°C for 15 min in the air, and the thickness of the PEDOT:PSS layer is about 40 nm. The three different polymer donors and Y22 (1:1.2, 16 mg/mL in total concentration) were dissolved in CF and different ratio of additives and spin-cast at 2000 rpm for 40s onto the PEDOT:PSS layer. Thermal annealing treatment were performed under different temperatures with different time for the active layer. Then methanol solution of PDINO at a concentration of 1.0 mg mL^{-1} was deposited atop the active layer at 3000 rpm for 30 s to afford a PDINO cathode buffer layer. Finally, the metal cathode Al was thermally evaporated under a shadow mask with a base pressure of approximately 10^{-4} Pa. The active area of the OSCs is 4.6 mm^2 . All of these fabrications and

characterizations after spin-coated PEDOT:PSS substrates were conducted in a glove box.

2.2.3 Hole-only devices

The structure for hole-only devices is ITO/PEDOT: PSS/active layer/MoO₃/Al. A 30 nm thick PEDOT: PSS layer was made by spin-coating an aqueous dispersion onto ITO substrates (4000 rpm for 30 s). PEDOT substrates were dried at 150 °C for 15 min. A blend film in CF was spin-coated onto PEDOT layer. Finally, MoO₃ (~6 nm) and Ag (~80 nm) was successively evaporated onto the active layer through a shadow mask (pressure under ca. 10⁻⁴ Pa). *J-V* curves were measured by using a computerized Keithley 2400 Source Meter in the dark.

2.2.4 Electron-only devices

The structure for electron-only devices is ITO/ ZnO/active layer/PDINO/Al. ZnO was evaporated onto a ITO glass substrate. A PM6:Y22 blend in CF was spin-coated onto ZnO. PDINO was spin-coated onto active layer and Al (~80 nm) was successively evaporated onto the active layer through a shadow mask (pressure under ca. 10⁻⁴ Pa). *J-V* curves were measured by using a computerized Keithley 2400 Source Meter in the dark.

2.3 Optimization of Device Performance

Table S1 Optimization of D/A ratio for PM6:Y22 inverted solar cells.^a

Ratio	V_{oc} (V)	J_{sc}	FF (%)	PCE (%) ^b
1:1	0.864	22.91	74.43	14.74 (±0.12)

)
1:1.2	0.851	23.16	74.71	14.72	(±0.10)
)
1:1.4	0.845	23.27	73.73	14.49	(±0.16)
)
1:1.8	0.837	23.32	72.44	14.14	(±0.24)
)

^a Blend solution: 16 mg/mL in CF with 0.5 vol % CN; spin-coating: 1500 rpm for 60 s; the active layer with 5 min thermal annealing at 100 °C.

^b Data in parentheses stand for the average PCEs for 20 cells.

Table S2 Optimization of CN content for PM6:Y22 inverted solar cells.^a

Ratio	Additive	V_{oc} (V)	J_{sc}	FF (%)	PCE (%) ^b
1:1.2	CN, 0.2%	0.853	22.88	76.91	15.02(±0.19)
	CN, 0.3%	0.853	24.37	74.12	15.40(±0.31)
	CN, 0.5%	0.853	22.33	76.44	14.55(±0.11)
	CN, 0.8%	0.849	21.66	76.63	14.25(±0.10)

^a D/A ratio: 1:1.2 (w/w); blend solution: 16 mg/ mL in CF; the active layer with 5 min thermal annealing at 100 °C.

^b Data in parentheses stand for the average PCEs for 20 cells.

Table S3 Optimization of different donors for donor:Y22 in inverted solar cells.^a

Donor	V_{oc} (V)	Additive (%)	J_{sc}	FF (%)	PCE (%) ^b
PM6	0.853	0.3, CN	24.37	74.12	15.40(±0.31)
QX2	0.785	0.5, CN	23.76	68.07	12.69(±0.38)
J71	0.806		21.70	62.27	10.89(±0.26)

^a D/A ratio: 1:1.2 (w/w); blend solution: 16 mg/mL in CF; the active layer with 5 min thermal annealing at 100 °C.

^b Data in parentheses stand for the average PCEs for 20 cells.

Table S4 Optimization of different temperature for PM6:Y22 inverted solar cells.^a

Ratio	Annealing (°C)	V_{oc} (V)	J_{sc}	FF (%)	PCE (%) ^b
1:1.2	60	0.863	22.84	76.11	15.00(±0.16)
	80	0.859	22.48	76.43	14.76(±0.08)
	100	0.853	22.88	76.91	15.02(±0.19)

^a D/A ratio: 1:1.2 (w/w); blend solution: 16 mg/mL in CF; the active layer with 5 min thermal annealing at different temperatures.

^b Data in parentheses stand for the average PCEs for 20 cells.

Table S5 Photovoltaic characteristics of conventional OSCs with ITO/PEDOT:PSS/PM6:Y22/ PDINO /Al^a

Ratio	Annealing (°C)	Additive (%)	V_{oc} (V)	J_{sc}	FF (%)	PCE (%) ^b
1:1	100 ,5min	CN (0.5)	0.863	22.57	75.72	14.75(±1.42)
	100 ,5min	/	0.873	22.66	70.92	14.03(±1.79)
	/	CN (0.5)	0.876	22.58	74.33	14.70(±1.08)
	/	/	0.888	21.81	66.10	12.80(±0.29)

^a D/A ratio: 1:1 (w/w); blend solution: 16 mg/mL in CF with different additions.

^b Data in parentheses stand for the average PCEs for 20 cells.

Table S6 Photovoltaic characteristics of inverted OSCs with ITO/ZnO/PM6:Y22/MoO₃/Ag^a

Ratio	Annealing (°C)	Additive(%)	V_{oc} (V)	J_{sc}	FF(%)	PCE(%) ^b
1:1.2	100, 5 min	CN (0.3)	0.853	24.37	74.12	15.40(±0.31)
	–	–	0.822	21.81	66.66	11.96(±0.12)

^a D/A ratio: 1:1.2 (w/w); blend solution: 16 mg/mL in CF.

^b Data in parentheses stand for the average PCEs for 20 cells.

2.4 Additional Information

Table S7 Optical properties and electronic energy levels of Y22 and PM6.

	λ_{max}^{abs} [nm]		λ_{onset}	E_g^{optc}	E_{HOMO}^a	E_{LUMO}^b	E_g^{cv}
	Solution	Film	[nm]	[eV]	[eV]	[eV]	[eV]
Y22	743	826	900	1.38	-5.69	-3.94	1.75
PM6	550	614	690	1.80	-5.45	-3.65	1.80

${}^a E_{\text{HOMO}} = -(4.80 - E_{\text{ox,Fc/Fc}^+} + E_{\text{ox}})$ (eV), ${}^b E_{\text{LUMO}} = -(4.80 - E_{\text{red,Fc/Fc}^+} + E_{\text{red}})$ (eV) using Ag/AgCl as the reference electrode.

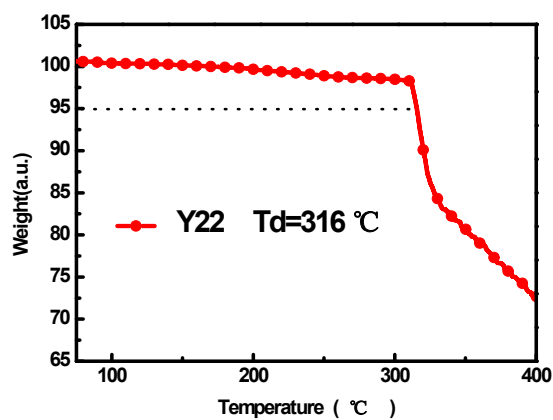


Figure S1 Thermogravimetric analysis curve of Y22 with heating rate of 20 °C min⁻¹.

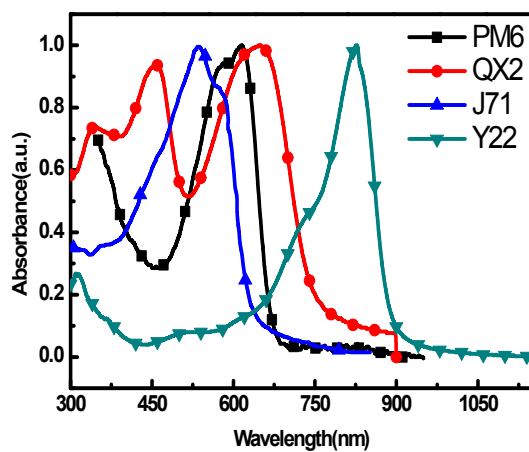


Figure S2 The absorption spectra of three different polymer donors and Y22 in the thin film states.

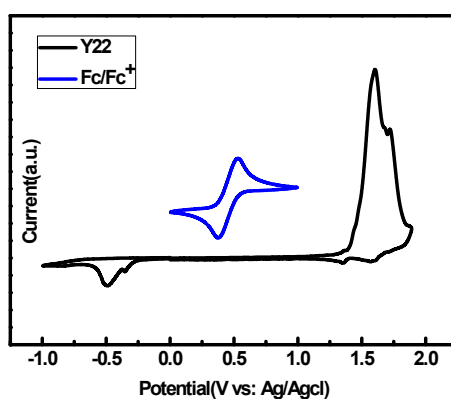


Figure S3 The cyclic voltammogram of Y22 in CH₃CN/0.1MBu₄NPF₆.

Table S8 Hole mobility and electron mobility of PM6:Y22 based BHJ film by SCLC method.

Device	μ_h (cm ² ·V ⁻¹ ·s ⁻¹)	μ_e (cm ² ·V ⁻¹ ·s ⁻¹)	μ_e/μ_h
Optimized	10.88×10^{-4}	9.99×10^{-4}	0.92
As cast	6.58×10^{-4}	4.77×10^{-4}	0.72

Table S9 A summary of excellent performance reported asymmetric fullerene-free acceptors with high J_{sc} ($J_{sc} > 15$ mA cm⁻²) and high performance (PCE > 10%).

NFAs	E_g^{opt} (eV)	HOMO/ LUMO (eV)	Donor	J_{sc} (mA/cm ²)	V_{oc} (V)	FF (%)	PCE (%)	Reference
TPTT- IC	1.63	-5.78/ -3.95	PBT1-C	15.6	0.96	70	10.5	J. Mater. Chem. C, 2016, 4873

IDT6C N-M	1.65	-5.60/ -3.87	PBDB-T	16.02	0.91	76.83	11.20	Adv. Mater. 2018, 30, 1800052
IDT6C N-Th	1.61	-5.71/ -4.01	PBDB-T	16.75	0.81	76.72	10.41	Adv. Mater. 2018, 30, 1800052
TPTT- 2F	1.58	-5.75/ -4.04	PBT1-C	15.82	0.88	73	10.17	J. Mater. Chem. A 2018, 6, 18847.
TPTTT- 2F	1.56	-5.69/ -4.01	PBT1-C	17.63	0.91	74.5	12.03	J. Mater. Chem. A 2018, 6, 18847.
TTPTT T-2F	1.54	-5.67/ -4.04	PBT1-C	16.78	0.92	74.6	11.52	Sol. RRL 2019, 3, 1800246.
TTPTT T-4F	1.52	-1.69/ -4.12	PBT1-C	19.36	0.86	72.1	12.05	Sol. RRL 2019, 3, 1800246.
IDT8C N-M	1.58	-5.54/ -3.91	PBDB-T	17.11	0.92	78.9	12.43	ACS Energy Lett. 2018, 3, 1760- 1768.
MeIC1	1.54	-5.59/ -3.89	PBDB-T	18.32	0.92	74.1	12.58	Chem. Sci. 2018, 9, 8142
SePT- IN	1.54	-5.77/ -4.00	PBT1-C	16.37	0.85	73.3	10.20	J, Energy Chem. 2020, 40, 144.
SePTT- 2F	1.50	-5.71/ -4.00	PBT1-C	17.51	0.83	75	10.09	J. Mater. Chem. A, 2019, 7, 1435
SePTTT	1.50	-5.66/ -4.00	PBT1-C	18.02	0.89	75.9	12.24	J. Mater. Chem. A,

-2F		-3.97						2019, 7, 1435
IDT-OB	1.66	-5.77/ -3.87	PBDB-T	16.18	0.88	71.1	10.12	Adv. Mater. 2017, 29, 1703527
IDTT-OB	1.59	-5.59/ -3.88	PBDB-T	16.58	0.91	74	11.19	ACS Appl. Mater. Interfaces 2019, 11, 3098
IDTT-2F-Th	1.55	-5.78/ -4.09	PBT1-C- 2Cl	17.82	0.91	73.9	12.01	J. Mater. Chem. A 2019, 7, 8055
ITIC-2F	1.56	-5.76/ -4.07	PBDB- TF	17.3	0.92	65.7	10.38	J. Am. Chem. Soc. 2019,141, 3274.
ITIC-3F	1.54	-5.73/ -4.12	PBDB- TF	19.4	0.89	66.5	11.44	J. Am. Chem. Soc. 2019,141, 3274.
a-IT-2OM	1.63	-5.61/ -3.92	PBDB	18.11	0.93	71.52	12.07	J. Mater. Chem. A, 2019, 7, 8889– 8896
a-IT-2F	1.56	-5.67/ -4.07	PBDB	19.06	0.78	68.84	10.28	J. Mater. Chem. A, 2019, 7, 8889– 8896
IT-3F	1.54	-5.67/ -4.09	PBDB- TF	20.35	0.93	75.5	13.83	J. Mater. Chem. A, 2019, 7, 8889– 8896
ITIC-2F	1.50	-5.64/ -4.07	PBDB- TF	20.67	0.90	71.53	12.31	J. Mater. Chem. A

		-3.76						2018, 6, 22519.
a- BTTIC	1.43	-5.60/ -3.86	PBDB-T	20.31	0.90	74	13.6	J. Mater. Chem. A 2019,7,11053- 11061
IPT-2F	1.44	-5.51/ -3.96	PBDB-T	22.40	0.86	72.4	14.0	J. Mater. Chem. A, 2019,7,22279– 22286
IPTT-2F	1.42	-5.46/ -4.04	PBDB-T	19.70	0.87	66.2	11.4	J. Mater. Chem. A, 2019, 7, 22279 –22286
IPTTT- 2F	1.43	-5.40/ -4.07	PBDB-T	20.00	0.89	69.3	12.3	J. Mater. Chem. A, 2019,7,22279 –22286

7. Spectral Charts of NMR and MS

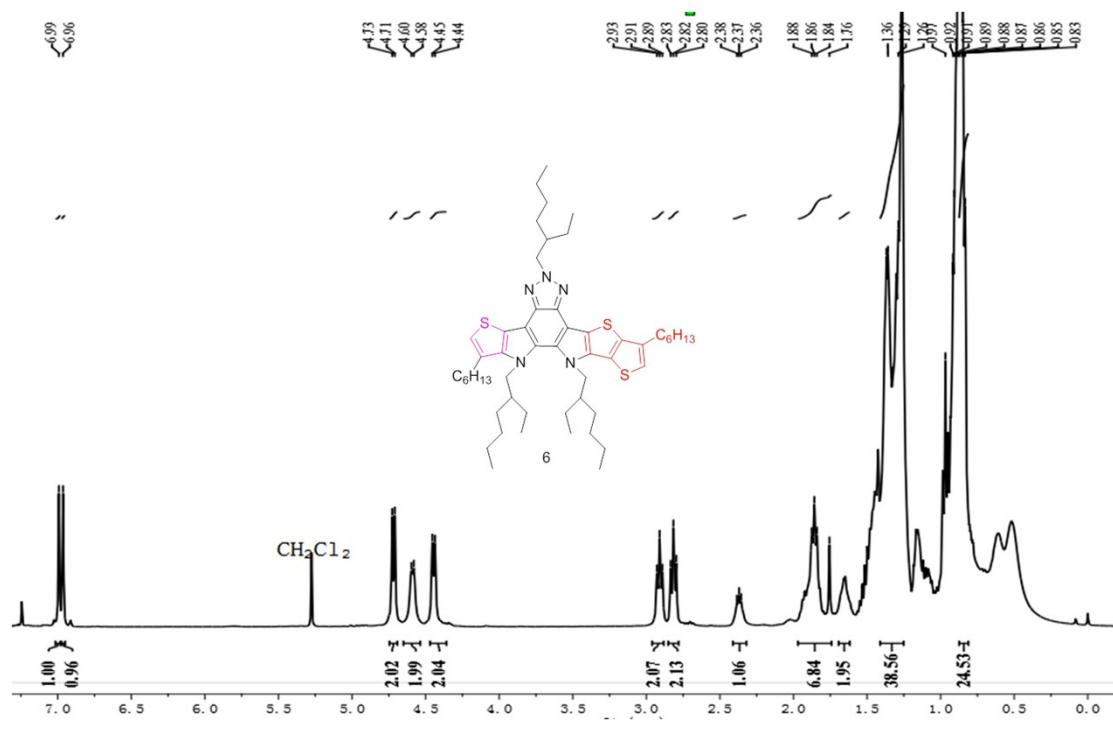


Figure S4 ¹H NMR spectrum of compound 6 in CDCl₃.

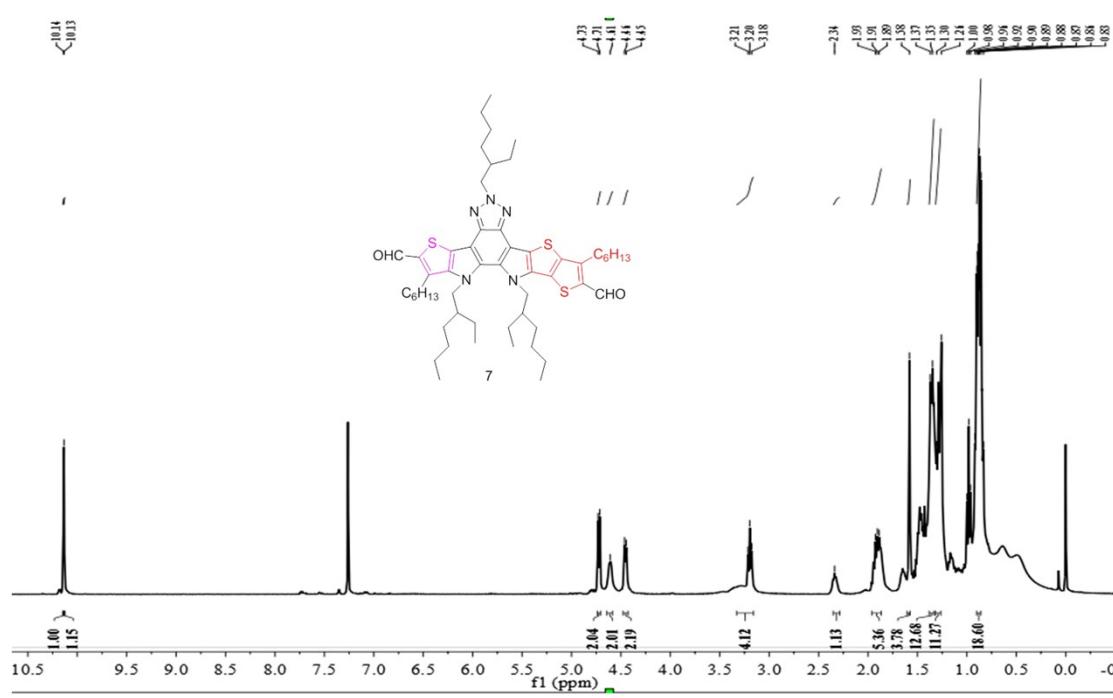


Figure S5 ¹H NMR spectrum of compound 7 in CDCl₃.

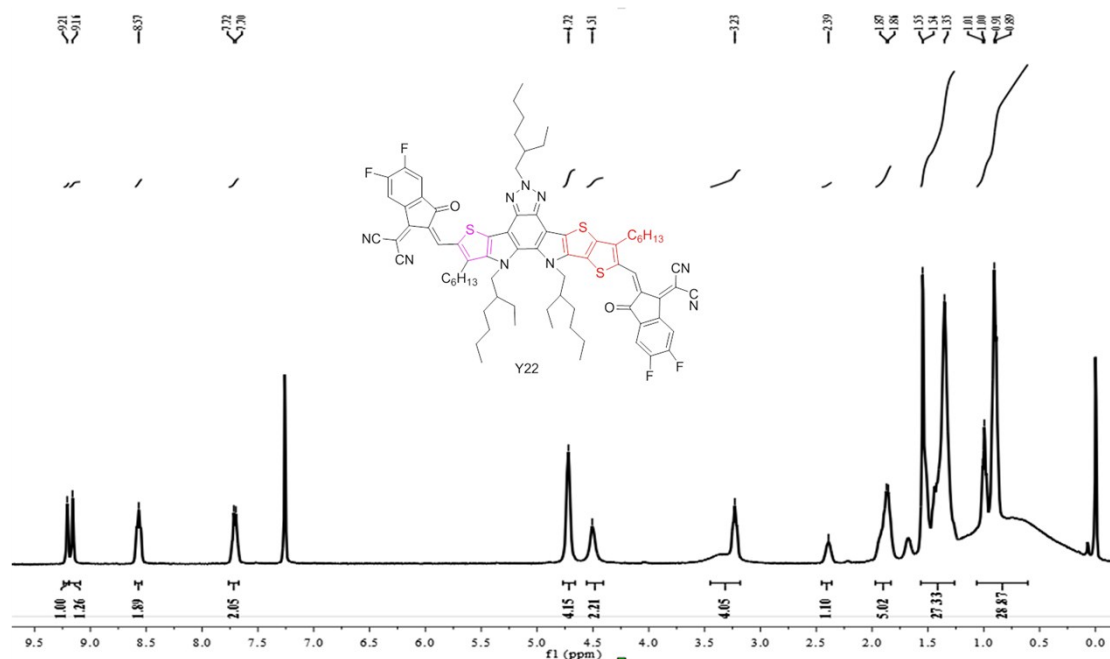


Figure S6 ^1H NMR spectrum of Y22 in CDCl_3 .

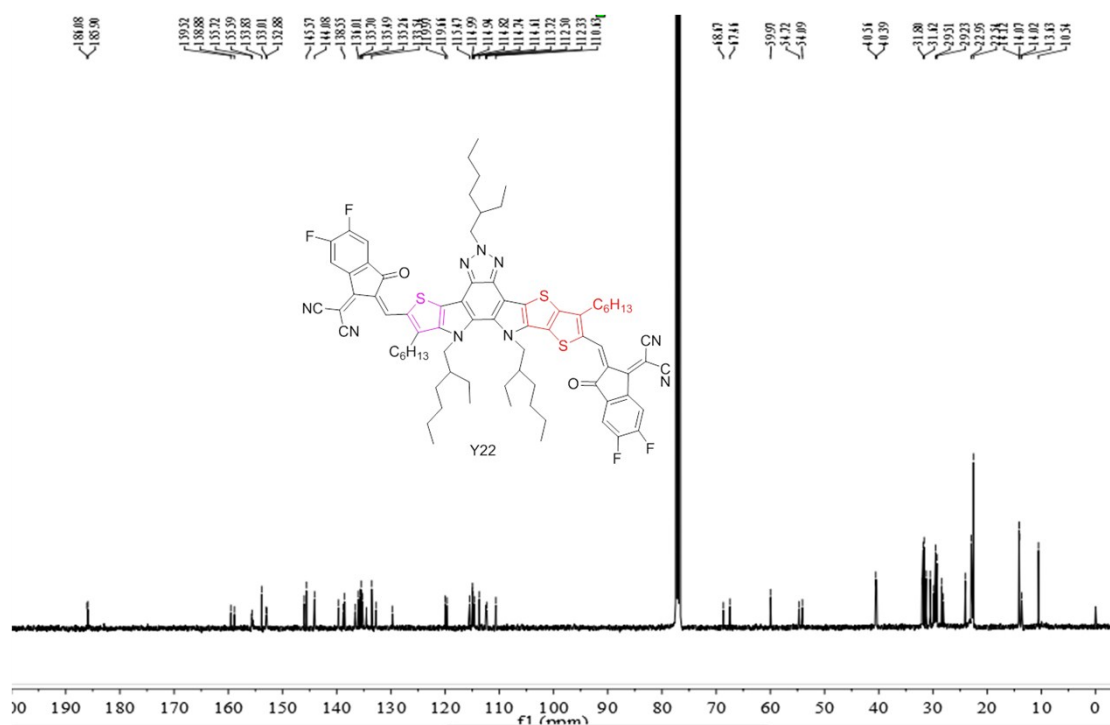


Figure S7 ^{13}C NMR spectrum of Y22 in CDCl_3 .

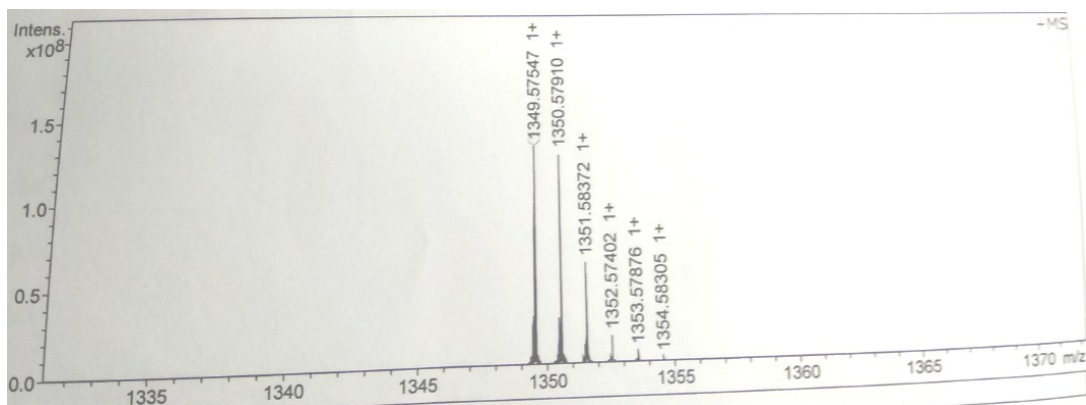


Figure S8 The high resolution mass spectrum (MALDI-TOF) of Y22.

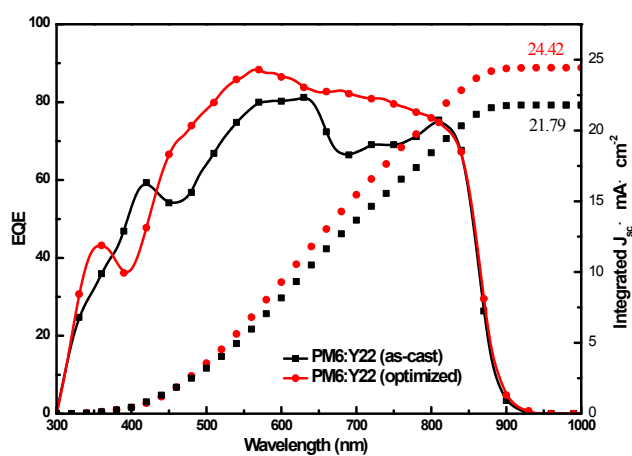
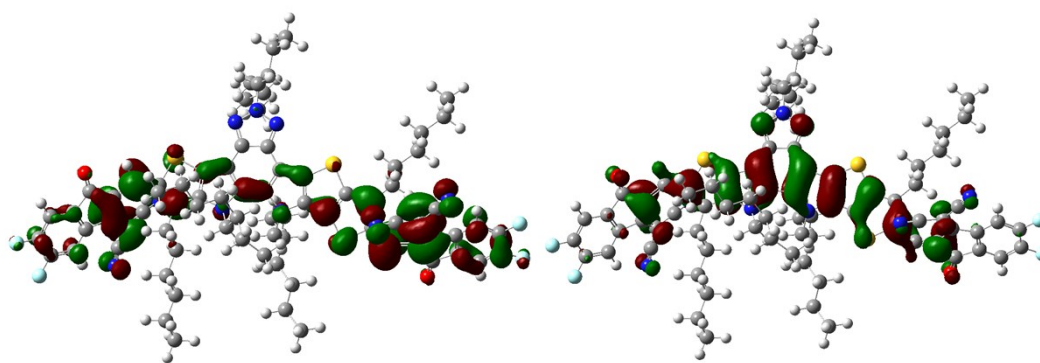


Figure S9. *EQE* curve for devices based on PM6:Y22.



LUMO: -3.65 eV

HOMO: -5.63 eV

Figure S10. LUMO and HOMO for Y22. Calculations were carried out by

DFT/B3LYP/6-31G (d, p).

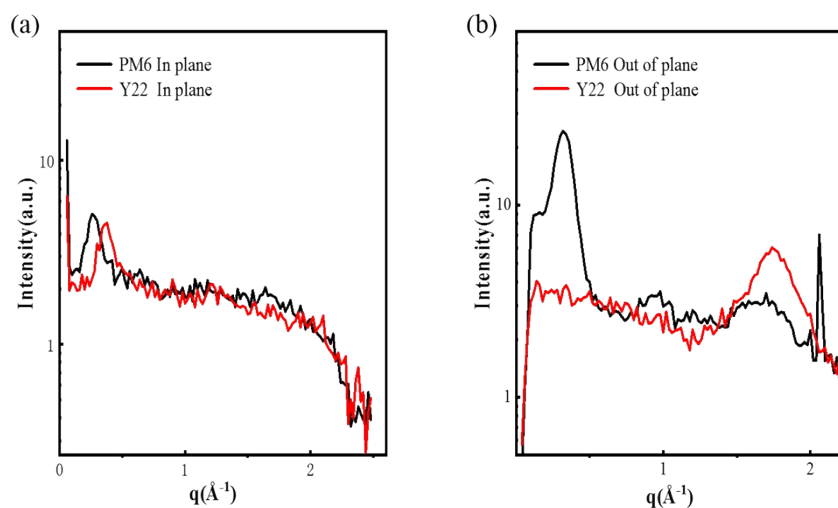


Figure S11. GIWAXS intensity profiles along the in-plane (a) and out-of-plane (b) directions of neat PM6 Y22 film.

References

1. J. Yuan, T. Huang, P. Cheng, Y. Zou, H. Zhang, J. L. Yang, S. Y. Chang, Z. Zhang, W. Huang, R. Wang, D. Meng, F. Gao and Y. Yang, *Nature communications*, 2019, **10**, 1624.
2. M. Luo, L. Zhou, J. Yuan, C. Zhu, F. Cai, J. Hai and Y. Zou, *Journal of Energy Chemistry*, 2020, **42**, 169-173.
3. J. Yuan, Y. Zhang, L. Zhou, C. Zhang, T. K. Lau, G. Zhang, X. Lu, H. L. Yip, S. K. So, S. Beaupre, M. Mainville, P. A. Johnson, M. Leclerc, H. Chen, H. Peng, Y. Li and Y. Zou, *Advanced materials*, 2019, **31**, e1807577.